https://doi.org/10.31436/iiumej.v25i2.3029

ENHANCING PROSTHETIC CONTROL: NEURAL NETWORK CLASSIFICATION OF THUMB MUSCLE CONTRACTION USING HD-SEMG SIGNALS

MUHAMMAD MUKLIS SUHAIMI, AIMI SHAZWANI GHAZALI*, AHMAD JAZLAN HAJA MOHIDEEN, MUHAMMAD HARIZ HAFIZALSHAH, SHAHRUL NA'IM SIDEK

Dept. of Mechatronics Engineering, International Islamic University Malaysia, Kuala Lumpur, Malaysia.

**Corresponding author: aimighazali@iium.edu.my*

(Received: 20 September 2023; Accepted: 31 October 2024; Published online: 14 July 2024)

ABSTRACT: The progression of prosthetic technology, enabling precise thumb control and movement, has reached a stage where noninvasive techniques for capturing bioelectrical signals from muscle activity are preferred over alternative methods. While electromyography's applications extend beyond just interfacing with prostheses, this initial investigation delves into evaluating various classifiers' accuracy in identifying rest and contraction states of the thumb muscles using extrinsic forearm readings. Employing a High-Density Surface Electromyogram (HD-sEMG) device, bioelectrical signals generated by muscle activity, detectable from the skin's surface, were transformed into contours. A training system for the thumb induced muscle activity in four postures: 0°, 30°, 60°, and 90°. The collection of HD-sEMG signals originating from both the anterior and posterior forearms of seventeen participants has been proficiently classified using a neural network with 100% accuracy and a mean square error (MSE) of 1.4923 x 10^{-5} based on the testing dataset. This accomplishment in classification was realized by employing the Bayesian regularization backpropagation (trainbr) training technique, integrating seven concealed layers, and adopting a training-validation-testing proportion of 70-15-15. In the realm of future research, an avenue worth exploring involves the potential integration of real-time feedback mechanisms predicated on the recognition of thumb muscle contraction states. This integration could offer an enhanced interaction experience between users and prosthetic devices.

ABSTRAK: Perkembangan teknologi prostetik mengguna pakai kaedah selamat iaitu isyarat bioelektrikal yang diperoleh dari pergerakan otot lebih digemari digunakan berbanding kaedah alternatif. Ini membolehkan kawalan dan pergerakan ibu jari dengan tepat. Sementara aplikasi elektromiografi telah melangkah jauh melebihi antara muka prostesis. Kajian awal ini mengkaji pelbagai ketepatan klasifikasi dalam mengenal pasti keadaan rehat dan kontraksi otot ibu jari menggunakan bacaan lengan bawah ekstrinsik. Dengan menggunakan peranti Elektromiogram Permukaan Kepadatan-Tinggi (HD-sEMG), isyarat bioelektrikal yang terhasil dari pergerakan otot, boleh ditanggalkan dari permukaan kulit, di ubah kepada kontur. Sistem latihan pada ibu jari menghasilkan pergerakan otot dalam empat postur iaitu: 0°, 30°, 60°, dan 90°. Isyarat terkumpul dari HD-sEMG berasal dari kedua-dua lengan tangan anterior dan posterior dari 17 peserta telah diklasifikasi dengan cekap menggunakan rangkaian neural dengan ketepatan 100% dan min kuasa dua ralat (MSE) sebanyak 1.4923 x 10-5 berdasarkan setdata yang diuji. Klasifikasi sempurna ini dicapai dengan menggunakan teknik latihan aturan rambatan-belakang Bayesian (trainbr), mengguna pakai tujuh lapisan tersembunyi dengan gabungan latihan-validasi-ujian mengikut kadar 70-15-15. Pada masa hadapan, pengkaji boleh menerokai potensi integrasi mekanisme tindak balas nyata dalam meramal dan

mengenali kontraksi otot ibu jari. Integrasi ini mungkin membolehkan pengalaman interaksi antara peranti prostetik dan pengguna.

KEYWORDS: *Thumb Posture, High-Density Surface Electromyogram (HD-sEMG), Forearm Muscle, Classification.*

1. INTRODUCTION

The human hand serves as the principal organ for tactile perception thanks to its high sensory receptor density. The hand performs a number of vital actions that are essential to human interaction and expression in everyday life, such as gripping for pick-up and holding mechanisms in addition to gesturing for nonverbal communication [1]. Executing complex motions that need coordination and precision like writing, relies on the intricate movements of hands, orchestrated by the muscles. For instance, gripping activities are created by the muscles in the hand, which include intrinsic muscles placed inside the hand and extrinsic muscles emerging from the forearm [2].

The absence of this vital biological component has a significant impact on an individual's freedom and general quality of life. As they adapt to their new surroundings, hand amputees frequently face physical, emotional, and mental challenges [3]. Significantly due to technological advancements, many hand amputees employ prosthetic devices to restore some level of hand function. Prosthetic technological advancements have resulted in the creation of sophisticated myoelectric prostheses that can be controlled by muscle impulses from the residual limb [4]. Amputees may use these prostheses to do a wide range of chores and activities, mimicking the capabilities of our natural hands.

There are different types of amputees, mainly transradial and transcarpal, distinguished by the extent of limb loss. Transradial amputees have forearms amputated between the elbow and wrist, losing the hand and wrist but keeping the elbow. This type of amputation affects the synergy between intrinsic and extrinsic hand muscles. On the other hand, transcarpal amputees lose part of the palm and wrist but retain some forearm and the wrist joint [5]. This type often preserves certain forearm muscles crucial for hand movements, making them the focus of this study since transcarpal amputees show potential for effective prosthetic use due to sustained forearm muscles capable of signaling specific hand movements [6].

In the context of prosthetic control, intrinsic and extrinsic muscles can be used to provide signals that direct the motions of a prosthetic hand, so increasing the device's utility and variety. Notably, the High-Density Surface Electromyogram (HD-sEMG) approach can detect muscle activity signals related to thumb movements using extrinsic muscles. HD-sEMG employs a larger number of electrodes to encompass a broader muscle area. The current state of prosthetic technology lacks precision, hindering its ability to address crucial aspects affecting users' daily lives [7]. This limitation hampers transcarpal amputees' ability to perform intricate movements essential for tasks involving grasping and manipulation. Moreover, HD-sEMG mitigates issues such as electrode misplacement that can occur with standard sEMG [8]. As a result, the imprecise thumb posture classification system from standard sEMG restricts transcarpal amputees from adapting to a wide range of tasks and activities. In general, there is a critical need for advancements in thumb posture classification from HD-EMG signals to revolutionize prosthetic control for transcarpal amputees, ensuring greater precision, functionality, and overall well-being for users [9].

A recent study has dedicated attention to optimizing the application of this technology to maximize the efficacy of HD-sEMG for hand gesture applications [10], while another

https://doi.org/10.31436/iiumej.v25i2.3029

combines the data collected with machine learning technique for classification purposes [11]. In line with this approach, a large dataset can be successfully handled by modern machine learning algorithms, combining with HD-sEMG's ability to collect large amounts of data. The first steps include feature extraction, which is a process of obtaining relevant information from the raw data provided by HD-sEMG. These features are classified into three types: time-domain (TD), frequency-domain (FD), and time-frequency domain (TFD). TFD analysis approaches find common ground in a variety of engineering fields, such as in gesture recognition purposes [12]. While frequency-based features (FD) have been employed due to their simple mathematical function (can be extracted using Fourier transformations) in earlier studies for healthcare purposes [13]. TD features have been widely used in previous research due to their superior performance in various fields such as in detecting sympathetic activity in post-acute COVID-19 patients [14], besides fault diagnosis of machines using vibration data [15]. This research is centered on time-domain (TD) features derived from the high-density surface electromyography (HD-sEMG) signals. This choice was informed by analyses conducted in a previous study [16], which advocated for the utilization of TD features, specifically emphasizing the inclusion of Root Mean Square (RMS) data, for effective biosignal feature extraction.

Based on the extracted features, the data are typically fed into machine learning for classification purposes. However, earlier studies have not treated the ratio of training, validation and testing in much detail. The research described in [17] used a 70-15-15 ratio in detecting healthy, myopathy, and neuropathy conditions based on the EMG signals in improving the evaluation of neuromuscular disorders. As per the performance assessment of the Convolutional Neural Network (CNN) approach, it attains a precision level of 98.57%. In another study as shown in [18], an 80-10-10 rule was employed to predict hand posture (pinch versus grip) and grasp force. The study utilized forearm sEMG and artificial neural networks (ANNs) during tasks that involved variations in repetition rate and duty cycle. The outcomes showed that overall accuracy for hand posture prediction was reported at 79%, while the overall accuracy for hand force prediction was recorded at 73%. In certain instances, a 60-20-20 split was utilized, as evidenced by a study with larger datasets consisting of 188 EMG signal data and 223 ECG signal data [19]. This approach was employed for muscle fatigue analysis and stress detection in the context of upper limb trauma rehabilitation. The outcomes revealed a remarkable 95% accuracy for multiclass muscle fatigue classification and a notable 97% accuracy during the binary classification of mental stress.

In this study, High-Density Surface Electromyogram (HD-sEMG) signals, derived from extrinsic forearm muscles situated on both the anterior and posterior sides, were utilized for classification purposes. During the experimental phase, participants were instructed to exert pressure on their thumb using a specifically designed platform. The thumb's posture was standardized at four different degrees. Employing a neural network developed within the Matlab environment, this study aims to reveal the highest accuracy achieved in classifying the extracted data.

Specifically, the study will assess the influence of forearm sides and thumb postures on HD-sEMG readings, considering three different training functions. Subsequent steps will involve exploring the optimal number of hidden layers for classifying the collected data, followed by selecting the best training-validation-testing ratios based on accuracy and mean square error (MSE).

https://doi.org/10.31436/iiumej.v25i2.3029

2. EXPERIMENTAL DESIGN

2.1 HD-sEMG Characteristics

HD-sEMG is a non-invasive measurement method for detecting muscle activity. The main difference between HD-sEMG and standard EMG is that HD-sEMG uses an array of closely spaced electrodes, which enables the detection of more detailed spatial muscle activity due to the large number of electrodes arranged in a dense manner. Standard EMG, on the other hand, typically uses a bipolar configuration consisting of two electrodes placed on the muscle of interest, enabling the detection of temporal muscle activity [23]. The ability to detect spatial muscle activity is advantageous in the development of prostheses. However, translating the HD-SEMG data into precise prosthetic hand movements remains a challenge. This section describes an experimental procedure for data collection to investigate the relationship between thumb movements/force exertion and forearm muscle activity.

2.2 Participants and Design

Seventeen students from the IIUM Gombak campus, aged 24 to 30 (with an average age of 26.35 and a standard deviation of 1.64), were chosen at random to participate in a within-subject experimental arrangement involving two conditions (relaxed vs. contracted) x four thumb postures (zero-degree vs. thirty-degree vs. sixty-degree vs. ninety-degree) for both forearm sides (anterior and posterior) across three trials based on RMS values. Prior to the start of the experiment, all participants were briefed on the experimental methods, after which they were granted their informed permission. The International Islamic University Malaysia (IIUM) approved the study protocol with the reference number 2020-080. There was no history of surgery, nerve damage, or accidents involving any of the individuals' dominant hands.

2.3 Task

Throughout the experimental session, all participants were instructed to engage their Maximum Voluntary Contraction (MVC) of thumb force using a portable thumb training device that had been developed (depicted in Fig. 1) in a neutral placement (at zero-degree position).

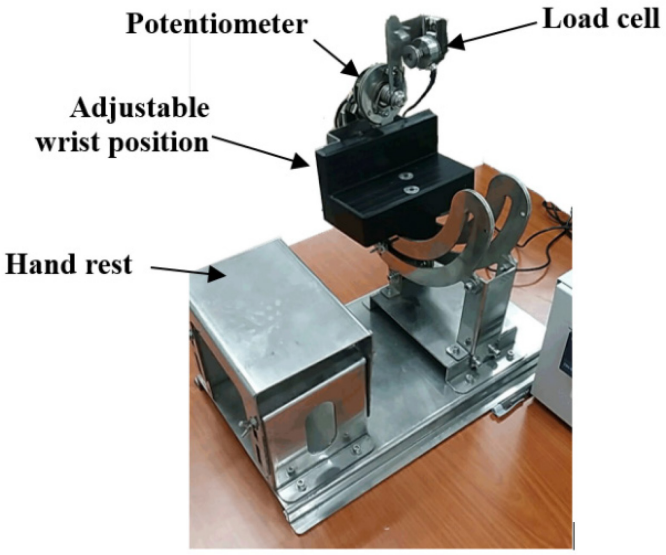

Figure 1. Thumb training platform (adopted from [5])

https://doi.org/10.31436/iiumej.v25i2.3029

The device included a potentiometer for detecting thumb posture arrangements, accompanied by a load cell for quantifying the force applied by participants. In addition, an adaptive wrist positioning system with a robust locking mechanism was designed to ensure accurate thumb position angles. A level hand rest was intended for participants to comfortably rest their arms during the experiment, effectively minimizing the potential onset of undue fatigue.

The thumb training platform was previously employed in a preceding study [16], albeit with slight adjustments made to establish a fixed angle configuration. For this experiment, angles of the thumb were set at zero-degree, thirty-degree, sixty-degree, and ninety-degree as shown in Fig. 2. Before the experiment, the experimenter set the dedicated angle by measuring the angle between the black base of the device and the tip of the load cell.

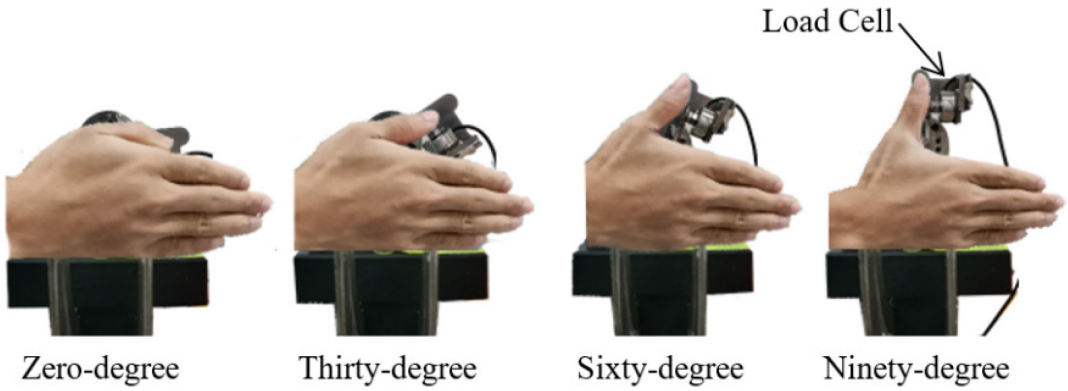

Figure 2. Thumb postures (adopted from [5])

Based on the integration of the Matlab program within the thumb training system, an automated process was employed to ascertain 30% of the MVC values for each thumb posture and subject, subsequently generating a corresponding graphical trajectory shown in Fig. 3.

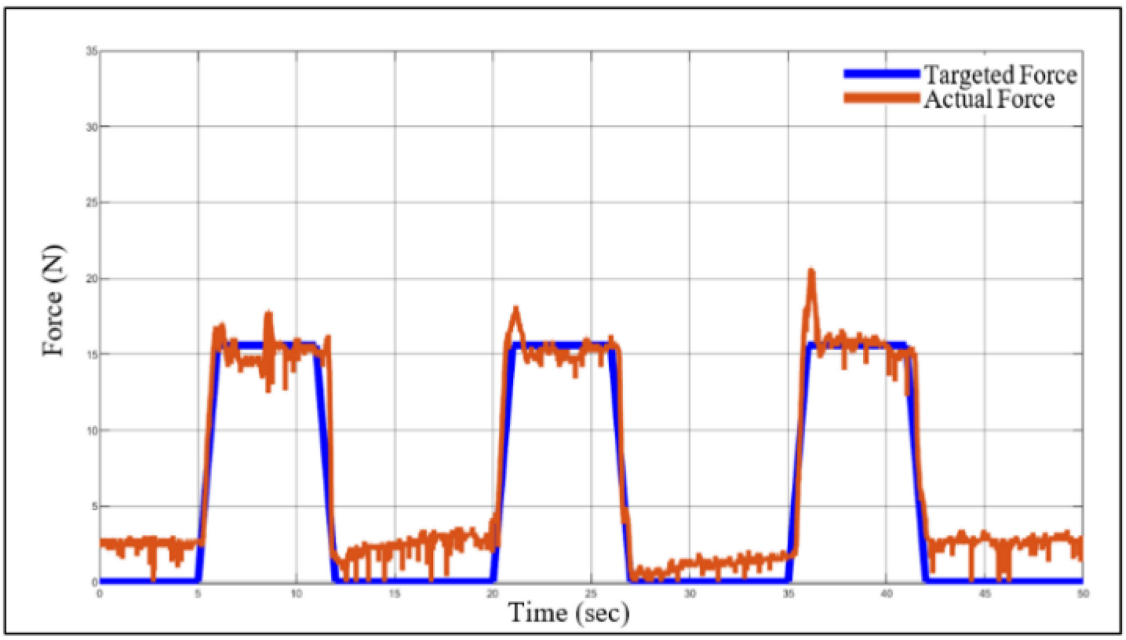

Figure 3. The trajectory of rest (force = 0 N) and contract (force= 30% MVC) conditions (adopted from [5])

https://doi.org/10.31436/iiumej.v25i2.3029

Utilizing the graphical user interface, participants engaged in repetitive cycles of resting and contracting positions for each trial. The blue line represents the targeted force, indicating the force that participants are required to exert, while the red line represents the actual force exerted by participants, measured by the load cell. This protocol encompassed three trials for every thumb posture, resulting in a total of nine contractile force measurements for each distinct thumb posture.

2.4 HD-sEMG Setting

HD-sEMG signals were captured using a portable biomedical signal amplifier (referred to as "Sessantaquattro") developed by OT-Bioelettronica . The electrode pad, organized in a grid pattern, consisted of 64 electrodes arranged in 5 columns and 13 rows, spaced 8mm apart. Following the methodology outlined in [20], the electrode pads were positioned on the anterior and posterior forearm, specifically at 25% of the previously measured full forearm length, counted from the ulnar head to the elbow crease. The positioning of the electrode in this study was also in line with a previous research [21], which found that the activation of the thumb is concentrated in the mid-forearm, adjacent to the radius bone.

Prior to affixing the patch onto participants' dominant forearm, a conductive gel was applied as a medium to ensure a secure connection between the skin and electrodes. This facilitated the direct transmission of electric impulses to the underlying tissues.

2.5 Procedure

Before beginning any experimental procedures, participants were given a consent form and instructed to read and complete it. After measuring each participant's forearm for patch placement purposes, the experimenter attached the electrodes to the forearm. Participants were then advised to sit up straight in a comfortable position before the data-collecting process began, as shown in Fig. 4.

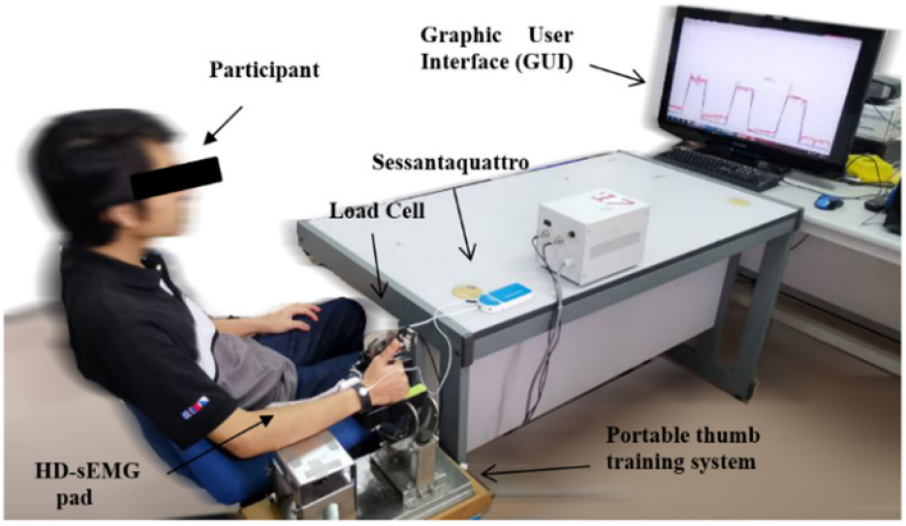

Figure 4. Experimental setup (adopted from [5])

Following that, instructions were given to the participants on how to place their arms on the portable thumb training device in a neutral posture (i.e., at a zero-degree angle). Participants were then directed to initiate their Maximum Voluntary Contraction (MVC) in order for MATLAB to calculate 30% of the MVC and generate the corresponding trajectory. This trajectory represented the force that participants had to apply over a certain period of time.

https://doi.org/10.31436/iiumej.v25i2.3029

Each trial required participants to match the anticipated trajectory by applying thumb force for five seconds, followed by an eight-second rest interval meant to reduce muscle strain. The experiment took around an hour to complete for all four thumb postures, following which the participants were debriefed by the experimenter. In recognition of their involvement, participants were provided with a monetary incentive at the end of the experiment.

2.6 Data processing

The collected data was subsequently extracted. A time-domain feature, which is RMS, was derived using software developed by OT-Bioelettronica. This feature computed through equation (1), encapsulating important aspects of the data.

$$RMS = \sqrt{\frac{1}{N}\sum_{k=1}^{N}(x_k)^2} \quad (1)$$

where N is the number of samples per window, and x_k is the amplitude of the signal of the amplifier input measured in mV. Note that, the samples per window were predefined at 1000 samples.

As each dataset was acquired from individual subjects exhibiting distinct characteristics, the process of normalization became imperative to address inter-subject variability. Normalization also helped in preventing bias due to domination of certain variables because of their greater magnitudes than others. The HD-sEMG signal data was subjected to normalization as per the formula depicted in equation (2).

$$\frac{n}{\bar{x}} \times 100\% \quad (2)$$

where $\bar{x}$ is the average of all normalized values, and n is n^{th} electrode's data out of the 64 electrodes.

3. RESULTS AND DISCUSSION

A total of 1632 data points were gathered for this study, comprising 2 conditions (contract vs. rest) x 4 angles (zero-degree vs. thirty-degree vs. sixty-degree vs. ninety-degree) x 3 trials for each condition x 4 readings (for each trial) x 17 participants. However, certain data from specific participants were excluded from the analysis due to grounding issues. Consequently, the dataset used for results encompassed 960 entries with 128 readings from the electrodes (64 electrodes each for posterior and anterior).

The data underwent classification using Matlab's neural network training. The selection of the training function was limited to Levenberg-Marquardt backpropagation (trainlm), Bayesian regularization backpropagation (trainbr), and Scaled conjugate gradient backpropagation (trainscg), depending on factors like classification speed and data size. Additionally, the neural network's hidden layer count was adjustable for better accuracy. Notably, the training, validation, and testing ratio was manually configured as suggested by earlier studies [22-24]. Lastly, customization of the classified data's performance was done, in which the neural network's performance was evaluated using the mean squared error value (MSE) [25].

To facilitate analysis, the data was divided into random segments (dividerand). 128 input nodes (64 electrodes x two forearm sides) were designed to classify the data into eight different classes (four thumb postures x two conditions), as detailed in Table 1.

https://doi.org/10.31436/iiumej.v25i2.3029

Table 1. Classes for neural network

Class	Condition	Thumb posture
1	Contract	Zero-degree
2		Thirty-degree
3		Sixty-degree
4		Ninety-degree
5	Relax	Zero-degree
6		Thirty-degree
7		Sixty-degree
8		Ninety-degree

In the first step, the number of hidden layers was temporarily set to one due to the small data size and the most popular 70-15-15 ratio was used for training-validation-testing. The outcomes indicated fluctuations in the Mean Squared Error (MSE) value for this setup. The configuration employing trainbr achieved the lowest error, which is at 0.0011, followed by trainlm at 0.0016, while trainscg exhibited the highest error at 0.1736.

For trainbr, the best training performance was 2.512×10^{-11} recorded at epoch 112. Further investigation was done to observe the receiver operating characteristic (ROC) of the classified data. The ROC can be interpreted as the closer each curve aligns with the left and upper boundaries of the plot, the more accurate the classification. While a true positive corresponds to a situation where the model accurately predicts the positive class, the false positive denotes an instance where the model mistakenly predicts the positive class. The findings depicted in Fig. 5 indicate elevated false positive rates in the testing ROC for two specific classes: Class 5 and Class 6. Conversely, the remaining classes exhibited no errors in this regard.

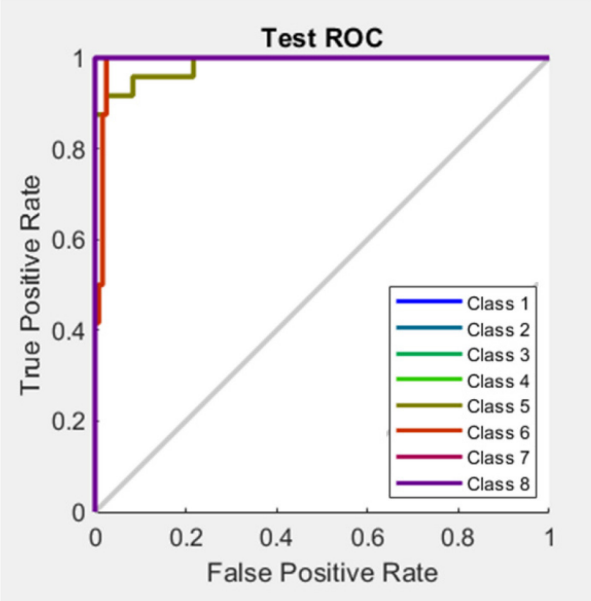

Figure 5. ROC for trainbr with 70-15-15 ratio

Derived from the confusion matrix of the testing subset, approximately 96.5% of the data was accurately classified. Amongst these, those two specific classes exhibited comparatively lower accuracy: 91.3% for Class 5 and 88.0% for Class 6. Taking into account the comprehensive confusion matrix, the collective rate of accurately classified data reached 99.5%.

https://doi.org/10.31436/iiumej.v25i2.3029

The second step of neural network analysis proceeded by varying the hidden layer size value, using trainbr function and still, a 70-15-15 ratio. Previous research presents divergent viewpoints regarding the optimal count of hidden layers. In [26], the recommendation leaned towards employing just one or two hidden layers to minimize neural network errors. Conversely, [27] proposed that utilizing five hidden layers adequately facilitated the classification of handwritten numerals. Consistent with the suggestions in [28] that advocated for trial-and-error approaches in determining hidden layer counts, [27] accentuated that augmenting the number of hidden layers led to a corresponding enhancement in the performance of the neural network under development.

Drawing from existing literature, alterations to the number of hidden layers were implemented in accordance with the details presented in Table 2. Furthermore, in alignment with the trial and error methodologies advocated in [28], the hidden layer configurations were diversified across multiple numbers to align with the classification's performance.

Table 2. MSE and % accuracy of the data based on the number of hidden layers

Hidden layer	MSE	% Correctly classified data (testing subset)
1	0.0011	96.5
2	0.0021	93.8
3	1.1943×10^{-4}	99.3
4	1.3852×10^{-4}	99.3
5	1.0235×10^{-4}	99.3
6	3.0434×10^{-5}	100
7	1.4923×10^{-5}	100
8	5.2345×10^{-4}	98.6

The escalation of hidden layers was capped at eight due to a decline in the neural network's performance. Specifically, when the hidden layer count was set at eight, both the MSE demonstrated an increase and the percentage of correctly classified data exhibited a decrease. Drawing insights from the outcomes presented in Table 2, a discernment can be drawn that the optimal hidden layer count for the given dataset amounted to seven. Additionally, it's notable that the computational time expanded with each increase in the hidden layer count. For instance, when the hidden layer count was set at five, the neural network required a mere 17 seconds to classify the data, whereas this time extended to a minute and 51 seconds when the hidden layer count was raised to eight.

Consequently, in the third phase of analysis, the training function was configured as 'trainbr', with the hidden layer count fixed at seven. Concurrently, variations were applied to the distribution of the training-validation-testing dataset ratios, encompassing both 80-10-10 and 60-20-20 settings. The findings indicated that with the 80-10-10 ratio, the neural network achieved a testing dataset classification accuracy of 97.9%, accompanied by an MSE of 5.2433x10-4. On the other hand, the 60-20-20 configuration yielded a classification accuracy of 99.0% and an MSE of 5.7381×10^{-4}.

As the 70-15-15 training-validation-testing ratio demonstrated superior classification accuracy in comparison to other ratios, additional analysis was conducted to delve into the finer aspects of this classification performance. The best training performance recorded was

https://doi.org/10.31436/iiumej.v25i2.3029

$1.3231x10^{-10}$ at epoch 105. Details of the performance for neural network training state can be seen in Fig. 6.

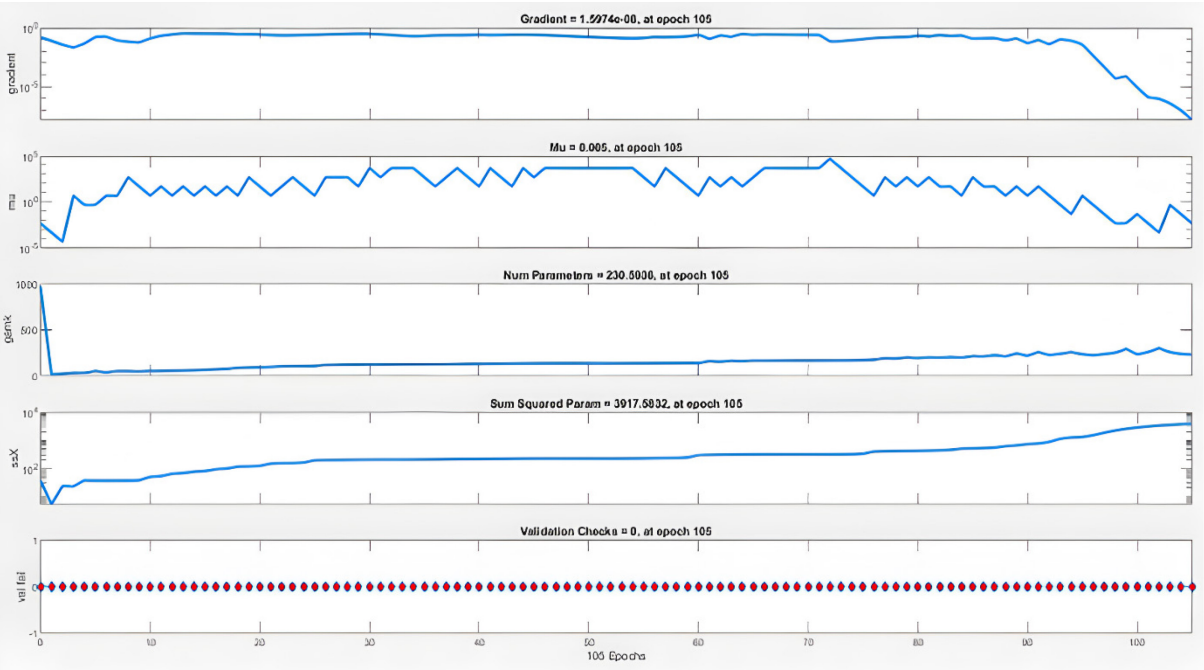

Figure 6. Training state performance for trainbr with seven hidden layers and 70-15-15 ratio

Furthermore, the comprehensive confusion matrix revealed a remarkable outcome, indicating that all data points, irrespective of their classes, were impeccably classified with a flawless accuracy of 100%. This exceptional classification achievement is corroborated by the ROC outputs depicted in Fig. 7.

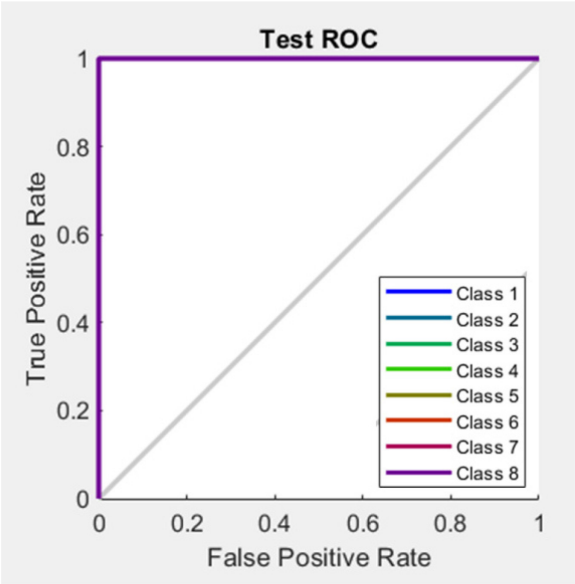

Figure 7. ROC for the configuration of trainbr with seven hidden layers and 70-15-15 ratio

4. CONCLUSION

The dataset comprising HD-sEMG signals obtained from the anterior and posterior forearm can indeed be effectively classified utilizing a neural network. This successful classification was achieved through the implementation of the Bayesian regularization backpropagation (trainbr) training function, incorporating seven hidden layers, and employing a training-validation-testing ratio of 70-15-15 with 100% accuracy classified data and 1.4923 $x10^{-5}$ MSE. Subsequent investigations could delve into assessing the adaptability and resilience of the established neural network classification model when confronted with variances in electrode positioning and user-specific variables. Such inquiries would further augment its pragmatic applicability. Moreover, broadening the scope of analysis to encompass more intricate hand movements and a wider array of muscle groups could provide valuable insights regarding the extended applicability of the HD-sEMG-based methodology.

REFERENCES

[1] A. R. Brown, W. Pouw, D. Brentari, and S. J. P. S. Goldin-Meadow, "People are less susceptible to illusion when they use their hands to communicate rather than estimate," vol. 32, no. 8, pp. 1227-1237, 2021.

[2] N. J. Jarque-Bou, J. L. Sancho-Bru, and M. J. S. Vergara, "A systematic review of emg applications for the characterization of forearm and hand muscle activity during activities of daily living: results, challenges, and open issues," vol. 21, no. 9, p. 3035, 2021.

[3] F. Kristjansdottir, L. B. Dahlin, H.-E. Rosberg, and I. K. J. J. o. H. T. Carlsson, "Social participation in persons with upper limb amputation receiving an esthetic prosthesis," vol. 33, no. 4, pp. 520-527, 2020.

[4] Z. Chen, H. Min, D. Wang, Z. Xia, F. Sun, and B. J. B. Fang, "A Review of Myoelectric Control for Prosthetic Hand Manipulation," vol. 8, no. 3, p. 328, 2023.

[5] M. M. Suhaimi, A. S. Ghazali, A. Jazlan, and N. J. C. E. Sidek, "Analysis of High-Density Surface Electromyogram (HD-sEMG) signal for thumb posture classification from extrinsic forearm muscles," vol. 9, no. 1, p. 2055445, 2022.

[6] E. L. Le, M. L. Iorio, M. A. J. E. J. o. O. S. Greyson, and Traumatology, "Targeted muscle reinnervation in upper extremity amputations," pp. 1-9, 2023.

[7] N. Parajuli *et al.*, "Real-time EMG based pattern recognition control for hand prostheses: A review on existing methods, challenges and future implementation," vol. 19, no. 20, p. 4596, 2019.

[8] P. M. Kloskowska, "The biomechanical determinants of sports related groin pain in athletes," Queen Mary University of London, 2016.

[9] A. Asghar, S. Jawaid Khan, F. Azim, C. S. Shakeel, A. Hussain, and I. K. J. P. o. t. I. o. M. E. Niazi, Part H: Journal of Engineering in Medicine, "Review on electromyography based intention for upper limb control using pattern recognition for human-machine interaction," vol. 236, no. 5, pp. 628-645, 2022.

[10] X. Jiang *et al.*, "Optimization of HD-sEMG-based cross-day hand gesture classification by optimal feature extraction and data augmentation," vol. 52, no. 6, pp. 1281-1291, 2022.

[11] H. Duan, C. Dai, and W. J. M. P. i. E. Chen, "The Evaluation of Classifier Performance during Fitting Wrist and Finger Movement Task Based on Forearm HD-sEMG," vol. 2022, 2022.

[12] Y. Li, J. Li, P. Tu, H. Wang, and K. J. I. S. J. Wang, "Gesture Recognition Based on EEMD and Cosine Laplacian Eigenmap," 2023.

[13] S. Siecinski, P. S. Kostka, and E. J. Tkacz, "Time domain and frequency domain heart rate variability analysis on electrocardiograms and mechanocardiograms from patients with valvular diseases," in *2022 44th Annual International Conference of the IEEE Engineering in Medicine & Biology Society (EMBC)*, 2022, pp. 653-656: IEEE.

[14] F. Liviero *et al.*, "Persistent Increase of Sympathetic Activity in Post-Acute COVID-19 of Paucisymptomatic Healthcare Workers," vol. 20, no. 1, p. 830, 2023.

[15] S.-i. Kim, Y. Noh, Y.-j. Kang, S. Park, and B. J. J. o. t. C. S. E. I. o. K. Ahn, "Fault classification model based on time domain feature extraction of vibration data," vol. 34, no. 1, pp. 25-33, 2021.

[16] S. N. Sidek, M. R. Roslan, S. Sidek, and M. S. M. J. I. J. o. C. I. S. Khalid, "Thumb-tip force prediction based on Hill's muscle model using electromyogram and ultrasound signal," vol. 11, no. 1, pp. 238-247, 2018.

[17] E. Aguiar-Salazar *et al.*, "Intelligent Electromyograph for Early Detection of Myopathy and Neuropathy Using EMG Signals and Neural Network Model," in *Conference on Information and Communication Technologies of Ecuador*, 2022, pp. 32-45: Springer.

[18] M. Wang *et al.*, "Hand posture and force estimation using surface electromyography and an artificial neural network," vol. 65, no. 3, pp. 382-402, 2023.

[19] E. Kassaw, E. Worassa, K. Fetene, and G. Aboye, "Muscle Fatigue Analysis and Stress Detection from Surface EMG and ECG Using Deep Learning for Upper-Limb Trauma Rehabilitation," 2023.

[20] A. Aranceta-Garza and B. A. Conway, "Differentiating variations in thumb position from recordings of the surface electromyogram in adults performing static grips, a proof of concept study," vol. 7, p. 123, 2019.

[21] X. Bao, Y. Zhou, Y. Wang, J. Zhang, X. Lü, and Z. J. P. o. Wang, "Electrode placement on the forearm for selective stimulation of finger extension/flexion," vol. 13, no. 1, p. e0190936, 2018.

[22] M.-C. Lu *et al.*, "Automatic Classification of Slit-Lamp Photographs by Imaging Illumination," p. 10.1097, 2022.

[23] H. Gupta *et al.*, "A hybrid convolutional neural network model to detect COVID-19 and pneumonia using chest X-ray images," vol. 33, no. 1, pp. 39-52, 2023.

[24] W. Setiawan and R. Rulaningtyas, "Visual explanation of maize leaf diaseases classification using squeezenet and gradient-weighted class activation map," in *AIP Conference Proceedings*, 2023, vol. 2679, no. 1: AIP Publishing.

[25] S. M. Alardhi *et al.*, "Artificial neural network model for predicting the desulfurization efficiency of Al-Ahdab crude oil," in *AIP Conference Proceedings*, 2022, vol. 2443, no. 1: AIP Publishing.

[26] G. Panchal, A. Ganatra, Y. Kosta, D. J. I. J. o. C. T. Panchal, and Engineering, "Behaviour analysis of multilayer perceptrons with multiple hidden neurons and hidden layers," vol. 3, no. 2, pp. 332-337, 2011.

[27] S. Asthana, A. Pandit, A. J. I. J. o. S. Bahrdwaj, and Technology, "Analysis of Multiple Hidden layers vs. Accuracy in Performance using Back Propagation Neural network," vol. 10, no. 4, pp. 1-4, 2017.

[28] F. S. Panchal, M. J. I. J. o. C. S. Panchal, and M. Computing, "Review on methods of selecting number of hidden nodes in artificial neural network," vol. 3, no. 11, pp. 455-464, 2014.